

Spin lifetime in high quality InSb epitaxial layers grown on GaAs

K. L. Litvinenko,^{a)} L. Nikzad, J. Allam, and B. N. Murdin
Advanced Technology Institute, University of Surrey, Guildford GU2 7XH, England

C. R. Pidgeon
Department of Physics, Heriot-Watt University, Edinburgh EH14 4AS, Scotland

J. J. Harris, T. Zhang, and L. F. Cohen
Blackett Laboratory, Imperial College London, Prince Consort Road, London SW7 2BZ, England

(Received 23 January 2007; accepted 21 February 2007; published online 20 April 2007)

The spin relaxation in undoped InSb films grown on GaAs has been investigated in the temperature range from 77 to 290 K. Two distinct lifetime values have been extracted, 1 and 2.5 ps, dependent on film thickness. Comparison of this data with a multilayer transport analysis of the films suggests that the longer time (~ 2.5 ps at 290 K) is associated with the central intrinsic region of the film, while the shorter time (~ 1 ps) is related to the highly dislocated accumulation region at the film-substrate interface. Whereas previous work on InAs films grown on GaAs showed that the native surface defect resulted in an additional charge accumulation layer with high conductivity but very short spin lifetime, in InSb layers the surface states introduce a depletion region. We infer that InSb could be a more attractive candidate for spintronic applications than InAs. © 2007 American Institute of Physics. [DOI: 10.1063/1.2719017]

I. INTRODUCTION

Narrow-gap semiconductors (NGSs) have been extensively studied due to their importance for the development of long wavelength optoelectronic devices and infrared detectors. InSb has been of particular interest, because of the recent development of extraordinary magnetoresistive sensors,¹ high speed electronic transistors,² and possible hybrid spintronic devices based on high mobility InSb epilayers.³ Moreover, a small electron effective mass as well as strong spin-orbit coupling, and hence a strong Rashba effect, make InSb a promising candidate for spintronic application.

It is essential for spintronics to be able to control spin dynamics with an external electric field.⁴ In bulk n -type semiconductors, two spin relaxation processes are dominant. They are described by the D'yakonov-Perel'⁵ (DP) and Elliot-Yaffet⁶ (EY) mechanisms. Only in the case of the DP process is it possible to alter the spin lifetime with an applied electric field by modulating the strength of the spin-orbit coupling through the Rashba effect. The efficiency of the DP mechanism is proportional to the electron mobility, whereas for the EY mechanism it is inversely proportional. It has been theoretically predicted that for bulk III-V semiconductors the EY process dominates only at very low temperature. Although the EY process is more effective for NGS, the transition between the DP and EY processes for high mobility InSb has been estimated to occur at 5 K.⁷ The situation is different in the case of low electron mobility. For low mobility InSb quantum wells (QW) it has already been reported that the crossover between the two processes could occur even at room temperature.⁸

From a practical point of view, InSb epilayers are gen-

erally grown on semi-insulating GaAs substrates. The lattice mismatch (14.6%) results in the formation of an interface accumulation layer with a large defect concentration, which is the main obstacle to the manufacturing of thin InSb films of high mobility. The electron mobility in this layer could be several orders of magnitude smaller than that in bulk material. Due to native surface defects, a low-barrier depletion region is formed on the surface of the InSb films. It has been suggested that the existence of an inversion layer at the surface would be preferable to form a contact with metallic materials without a significant resistance mismatch, and consequently, to increase the efficiency of spin injection from ferromagnetic materials.⁹ Charge accumulation is particularly strong on the surface of InAs (Ref. 10) and $\text{Hg}_{1-x}\text{Cd}_x\text{Te}$,¹¹ but as pointed out in our previous publication on InAs,⁹ the very short spin lifetime in this region is likely to be detrimental in lateral devices where current flows along the surface. Consequently, we have explored the spin relaxation properties of InSb films of various thicknesses to determine the optimum structure for spintronic applications.

Although the density and mobility profiles are expected to be gradually varying, for simplicity InSb films grown on GaAs have been considered as consisting of three regions: a surface depletion region, a low mobility interface, and a high mobility bulklike region. Because of the strong dependence of the spin relaxation processes on the mobility and carrier concentration, the transport properties and spin dynamics are different in these layers. For InAs films grown on GaAs substrates it was found that even for a thick film (1 μm), the majority of the current (60%) flows through the surface accumulation layer, which demonstrated a subpicosecond spin lifetime.⁹ It was pointed out in Ref. 9 that this fact means that if InAs is to be useful for spintronic applications steps must be taken to overcome the surface conduction. In contrast, InSb films have all the advantages of narrow-gap ma-

^{a)}Electronic mail: k.litvinenko@surrey.ac.uk

TABLE I. The depth-dependent electrical properties of the layers of the InSb films deduced from the differential model. i is the number of the layer ($i=0$ corresponds to the LT buffer layer), d the width of the layer, and x the relative amount of the total current flowing through the layer for a $1\ \mu\text{m}$ thick film. The 100 nm, 300 nm, and $1\ \mu\text{m}$ films consist of the first two, three, and four layers, respectively.

i	0	1	2	3
d (nm)	20	100	200	700
μ ($\text{m}^2/\text{V s}$)	0.035	0.85	1.5	4.2
n ($10^{-16}\ \text{cm}^{-3}$)	49	4.9	3.9	1.6
x (%)	≈ 0.5	≈ 7	≈ 18.5	≈ 74

materials, but without the complication of the surface layer, so that their electron transport properties could be adequately described by a two-channel model.¹²

In this work we have investigated the influence of the low mobility layers on the spin dynamics in InSb films. Three high quality undoped InSb films of thicknesses 0.1, 0.3, and $1\ \mu\text{m}$ were grown on semi-insulating GaAs (100)-oriented substrates (AXT) with a 20 nm low temperature (LT) grown InSb buffer, in a VG Semicon V80 molecular beam epitaxy (MBE) system. The improved two-step growth recipe with the LT buffer has been developed in Imperial College in order to reduce the influence of the defects originating at the interface of the InSb films.¹³ The samples were then annealed at a high temperature (HT). An additional investigation was performed to optimize the temperature of the HT second growth step, which was found to be $380\ \text{C}$.¹⁴ A remarkable improvement of the transport properties has been reported for these samples.¹⁴ For comparison, the spin relaxation of an undoped, $4\ \mu\text{m}$ thick InSb film (sample me1655) was also investigated. The mobility and carrier concentration of this film were $6.37\ \text{m}^2/\text{V s}$ ($3\ \text{m}^2/\text{V s}$) and $1.4 \times 10^{15}\ \text{cm}^{-3}$ ($2.8 \times 10^{15}\ \text{cm}^{-3}$) at 300 K (77 K), appropriate for the phonon limited mobility in quasibulk InSb.¹⁵

II. EXPERIMENTAL DETAILS AND RESULTS

In order to obtain the mobility μ and carrier concentration n , Hall measurements were performed on 5 mm diameter clover-leaf Van der Pauw patterns in the temperature range from 77 to 300 K. A detailed investigation of the transport properties of this set of high quality InSb films of different thicknesses is presented elsewhere.^{13,14,16} It was found that the transport properties of the films are well described by a two-channel conductivity model considering only the interface and bulklike region.¹⁶ In order to deconvolute the depth dependence of the mobility and carrier concentration from any pair of films in the set, it was assumed that the properties of the thinner film and the region of the same thickness of the thicker film are the same. Thus the properties of the remaining top region of the thicker film can be found differentially by means of the standard two-layer Hall formulas.¹⁴ The differential mobility and carrier concentration of these layers of the InSb films at room temperature are presented in Table I. Note that the layers $i=0, 1, 2,$ and 3 do not intentionally correspond to the interface, bulk, and surface regions discussed above, they simply represent the average carrier density and mobility over a specific region of

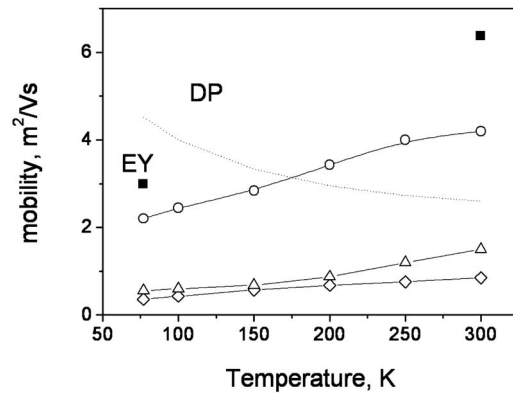


FIG. 1. Temperature dependence of the derived mobility of the layers, deduced by two-channel differential analysis of the set of InSb films: 100 nm layer (diamonds), 200 nm layer (triangles), and 700 nm layer (circles). The parameters of each layer are presented in Table I. The crossover mobility between the DP and EY processes is shown by the dotted line. The mobility of an undoped $4\ \mu\text{m}$ InSb film is shown by solid squares.

the film depth. However, Poisson-Schrödinger modeling of the band structure of these layers [see the inset, Fig. 3(b)] shows that the interface accumulation layer thickness and surface depletion depth (for low-doped material) are about 50 and 100 nm, respectively, so that to a good approximation the interface accumulation region consists of the LT layer ($i=0$) and first layer ($i=1$), and the surface depletion region is a small fraction of the third layer ($i=3$), the rest of which, along with the second layer ($i=2$), are in the bulklike intrinsic region. The latter is not quite homogeneous and in fact shows a gradual improvement in properties with increasing thickness. The sheet conductivity of each layer is equal to the product μnd , where d is the thickness of the channel, and thus the ratio of the current carried by each channel to the total current through the whole film can be estimated. As one can see from Table I, in the thickest film ($1\ \mu\text{m}$) the interface (sum of $i=0$ and $i=1$ layers) of the InSb film, which we have found to have a short spin lifetime (see below), carries not more than 7.5% of the total current. Over 92% therefore flows through the bulklike material, which is much greater than for the InAs films⁹ where for the same thickness 10% of the current flows through the interface region and 60% flows in the surface accumulation layer. Clearly in thinner films the proportion of current carried in the accumulation layer(s) is greater, and this accounts for the change in relative strengths of the observed lifetimes in the samples of different thicknesses.

The temperature dependencies of the derived mobility of each conducting channel are shown in Fig. 1. The temperature at which the predicted crossover between EY and DP processes occurs for the nondegenerate case is also shown in this figure. For the degenerate case, which is relevant only for the 0.1 and 0.3 μm films, the mobility of all constituent layers is in the EY dominated regime over the whole temperature range. Although the concentration of defects was significantly reduced by the improved growth recipe for distances greater than 100 nm from the LT buffer layer,¹⁴ the electron mobility is too small to remove EY spin flip scattering and to make such thin films suitable for spintronic appli-

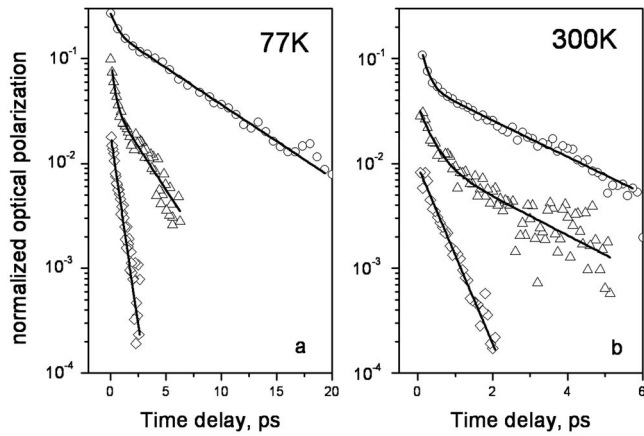


FIG. 2. Time evolution of the spin population measured at 77 K (a) and room temperature (b) for undoped InSb films of different thicknesses: 0.1 μm (diamonds), 0.3 μm (triangles), and 1 μm (circles).

cations at the room temperature. DP domination is only achieved at distances further than 300 nm from the interface.

A circularly polarized pump-probe experiment was performed to study the spin dynamics. The induced transmission change of the probe beam was measured as a function of the time delay between pump and probe pulses having the same circular polarizations (SCPs) and opposite circular polarizations (OCPs). The optical polarization (SCP–OCP)/(SCP+OCP) is proportional to the spin polarization in the sample.¹⁷ The light source was a difference frequency generator, which mixes the signal and the idler beams of an optical parametric amplifier, itself pumped by an amplified Ti:sapphire oscillator. The time resolution of the experiments was about 200 fs. A ZnSe photoelastic modulator was used to modulate the polarization of the pump beam. The detailed description of the experimental technique is given elsewhere.⁸ The energy of the photons was chosen to be close to the band gap in order to increase the penetration, so that we assume a uniform excitation through the thickness of the films.

As mentioned above, the mobility and carrier concentration gradually change with the depth of the films; nevertheless the evolution of the spin population, shown in Fig. 2 for all samples, can be well described by either a single or dual exponential decay.

III. DISCUSSION

As one can see from Fig. 2, the 0.1 μm film exhibits a single exponential spin decay for the whole temperature range, whereas the thicker films are found to have two exponential decays. The short component of the spin lifetimes has a similar value and temperature dependence for all samples and thus originate from the layers in common, i.e., the interface accumulation region. The intermediate thickness film (0.3 μm) exhibits two exponential decays, and the long component originates from layer $i=2$, i.e., the bulklike material. At 300 K the long lifetime contribution of layer $i=3$ in the thickest (1 μm) sample is similar to that of $i=2$. However, at 77 K there is a clear difference in the long lifetime components of the 0.3 and 1 μm films, and there is some evidence

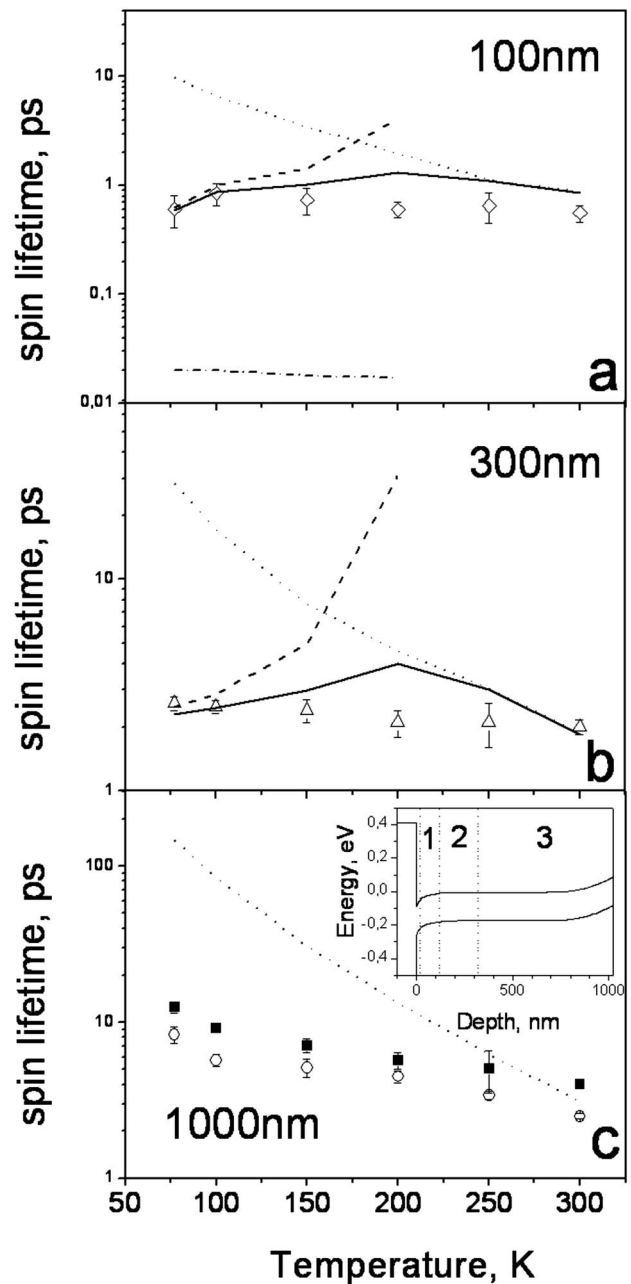


FIG. 3. The temperature dependence of the spin lifetime from the population decay curves. In the case of 0.3 and 1 μm films only the long components are shown. Also shown are the theoretical calculations of the spin lifetime for degenerate (dashed line), nondegenerate (dotted line), and Fermi-Dirac statistics (solid line). The estimated spin lifetime of the LT buffer layer is shown by the dashed-dotted line in Fig. 3(a) and the experimental spin lifetime of an undoped 4 μm thick InSb film by solid squares in Fig. 3(c). The Poisson-Schrödinger modeling of the band structure of the 1 μm film is shown in the inset (the numbers correspond to the HT layers in Table. I).

of the $i=2$ layer decay at short delay times in the signal from the 1 μm sample. The temperature dependencies of the spin lifetime of the 0.1 μm film as well as the long components of the spin lifetime of the other two samples are shown in Figs. 3(a)–3(c). The spin lifetime temperature dependence of the 4 μm , near-bulk InSb, also shown in Fig. 3(c), demonstrates that the top layer of the 1 μm film exhibits similar properties.

The mobility and carrier concentration of layers $i=1-3$ were used to calculate the spin lifetimes using degenerate and nondegenerate approximations. As expected from the mobility analyses, the spin lifetimes for 0.1 and 0.3 μm films are well described by the EY relaxation mechanism (see Figs. 3(a) and 3(b)). The DP process predicts a spin lifetime two orders of magnitude larger for these samples. For the 1 μm film the DP process dominates at room temperature, and the EY at low temperatures.

The DP spin relaxation rate in bulk materials is given by⁹

$$\frac{1}{\tau_s^{(\text{DP})}} \approx Q\beta^2 \frac{(E_k)^3}{\hbar^2 E_G} \tau_p, \quad (1)$$

where E_k is the electron kinetic energy, τ_p is momentum relaxation time, $\beta=(4\gamma/\sqrt{3-\gamma})(m_c/m_0)$, $\gamma=\Delta/(\Delta+E_G)$, Δ is the spin-orbit splitting of valence band, m_c/m_0 is the electron effective mass in units of the free mass, E_G is the fundamental energy gap, and Q is a dimensionless constant.

The EY spin relaxation rate is described by⁹

$$\frac{1}{\tau_s^{(\text{EY})}} \approx A\alpha^2 \left(\frac{E_k}{E_G}\right)^2 \frac{1}{\tau_p}, \quad (2)$$

where $\alpha=\gamma(1-\gamma/2)/(1-\gamma/3)$ and A is a dimensionless constant, the value of which depends on the orbital scattering mechanism.⁷ In the limit of degenerate statistics the typical electron kinetic energy E_k is given by E_F (the Fermi energy) and in the opposite limit of nondegenerate statistics, it is $k_B T$.

For the top layer of the 0.1 μm (0.3 μm) film the Fermi energy is approximately 26 meV (22 meV) at 77 K, but drops down to a few meV at room temperature. Therefore the transition from degenerate to nondegenerate statistics is within this temperature range. Both degenerate and nondegenerate cases are presented in Figs. 3(a) and 3(b). In order to obtain the spin lifetime in the intermediate regime, the average $\langle E_k^m \rangle$ is used to calculate the spin lifetime governed by both the DP ($m=3$) and EY ($m=2$) processes,⁹

$$\langle (E_k)^m \rangle = \frac{\int (E_k)^m f(E_k) \rho(E_k) dE_k}{\int f(E_k) \rho(E_k) dE_k}, \quad (3)$$

where $f(E)$ is the Fermi function, and ρ is the density of states. The result of this calculation is shown in Fig. 3 by solid lines. Only the nondegenerate case is shown for the 1 μm film. The values of A [Eq. (1)] and Q [Eq. (2)] were used as the only fitting parameters and were found to be $A=18$ for the 0.1 μm film [Fig. 3(a)], $A=9.5$ for the 0.3 μm film [Fig. 3(b)], and $A=9.5$ and $Q=1.5$ for the 1 μm film [Fig. 3(c)].

In order to estimate the spin lifetime of the low mobility, high carrier concentration LT buffer layer $i=0$ the degenerate EY relaxation mechanism was used, as shown in Fig. 3(a) by the dashed-dotted line. In spite of such a short spin lifetime, the LT buffer layer carries only 0.5% of the total current and therefore is not expected to affect the transport and spin properties of the films.

It should be mentioned that the spin lifetime in intrinsic bulk InSb under high intensity laser excitation, which we have previously reported to be 12 ps at room temperature,¹⁸

is three times larger than the spin lifetime presented in Fig. 3(c) for the sample me1655 under weak excitation. In Ref. 18 a free electron laser for infrared experiments (FELIX) was used to create the spin population. The peak energy of FELIX was about 1 μJ . Such intense laser pulses generated a significant photohole density, which more than doubled the spin lifetime.⁹ The peak energy of the laser pulses used in the experiment presented here was 10 nJ. The density of photoholes generated by such pulses is negligibly small in comparison with the FELIX experiment, and the measured spin lifetime is therefore the true electron spin DP lifetime, which was estimated in Ref. 18 to be about 6 ps or less. This value agrees very well with the 4 ps room temperature spin lifetime obtained in the present work and proves that with low energy laser pulses the real electron spin lifetime may be measured without the influence of photoholes.

IV. CONCLUSION

To summarize, we have measured the temperature dependence of the spin relaxation time in the range from 77 to 300 K for undoped InSb films of different thicknesses between 0.1 and 1 μm . The spin relaxation has several components, which corresponds very well with the model of inhomogeneous, layered conductivity. The spin lifetime in the interface accumulation layer was shown to be the subpicosecond value. Fortunately, its influence on the properties of the whole InSb film should not be significant, because the LT layer carries less than 1% of the total current in thick films. The rest of the accumulation layer, which was found to have a spin lifetime only a few times shorter than that in the bulk-like region, carries less than 7% of the total current and therefore will not considerably affect the properties of thick InSb films either. It was shown that the DP spin relaxation mechanism dominates in high mobility regions at room temperature, whereas the EY process dominates in low mobility regions over the whole temperature range and even in the high mobility regions at low temperature. The influence of the surface depletion layer was not detected in either the transport or spin properties of the films under investigation.

ACKNOWLEDGMENT

The EPSRC is acknowledged for financial support under Grant No. EP/C511999/1.

- ¹S. A. Solin, T. Thio, D. R. Hines, and J. J. Heremans, *Science* **289**, 1530 (2000).
- ²T. Ashley, A. B. Dean, C. T. Elliot, G. J. Pryce, A. D. Johnson, and H. Wills, *Appl. Phys. Lett.* **66**, 481 (1995).
- ³P. Murzin *et al.*, *Phys. Rev. B* **67**, 235202 (2003).
- ⁴K. C. Hall *et al.*, *Appl. Phys. Lett.* **86**, 202114 (2005); J. Nitta, T. Akazaki, and H. Takayanagi, *Phys. Rev. Lett.* **78**, 1335 (1997); T. Koga, J. Nitta, T. Akazaki, and H. Takayanagi, *ibid.* **89**, 046801 (2002).
- ⁵M. I. D'yakonov and V. I. Perel, *Sov. Phys. Solid State* **13**, 3023 (1972).
- ⁶R. J. Elliot, *Phys. Rev.* **96**, 266 (1954).
- ⁷P. H. Song and K. W. Kim, *Phys. Rev. B* **66**, 035207 (2002).
- ⁸K. L. Litvinenko *et al.*, *New J. Phys.* **8**, 49 (2006).
- ⁹K. L. Litvinenko *et al.*, *Phys. Rev. B* **74**, 075331 (2006).
- ¹⁰H. A. Washburn, J. R. Sites, and H. H. Wieder, *J. Appl. Phys.* **50**, 4872 (1979).
- ¹¹O. P. Agnihotri, C. A. Musca, and L. Faraone, *Semicond. Sci. Technol.* **13**, 839 (1998).
- ¹²T. A. Rawdanowicz, S. Lyer, W. C. Mitchel, A. Saxler, and S. Elhamri, *J.*

- Appl. Phys. **92**, 296 (2002).
- ¹³T. Zang, M. Debnath, S. K. Clowes, W. R. Branford, A. Bennett, C. Roberts, L. F. Cohen, and R. A. Stradling, *Physica E (Amsterdam)* **20**, 216 (2004).
- ¹⁴T. Zhang *et al.*, *Appl. Phys. Lett.* **84**, 4463 (2004).
- ¹⁵E. Litwin-Staszewska, W. Szymanska, and P. Piotrkowski, *Phys. Status Solidi B* **106**, 551 (1981).
- ¹⁶J. J. Harris, T. Zhang, W. R. Branford, S. K. Clowes, M. Debnath, A. Bennett, C. Roberts, and L. F. Cohen, *Semicond. Sci. Technol.* **19**, 1406 (2004).
- ¹⁷B. N. Murrin *et al.*, *Phys. Rev. B* **72**, 085346 (2005).
- ¹⁸B. N. Murrin *et al.*, *Phys. Rev. Lett.* **96**, 096603 (2006).